Dynamic encoding of social threat and spatial context in the hypothalamus

Piotr Krzywkowski[1,2], Beatrice Penna[1,3], and Cornelius T. Gross[1]*

[1] Epigenetics & Neurobiology Unit, EMBL Rome, European Molecular Biology Laboratory, Via Ramarini 32, 00015 Monterotondo (RM), Italy

[2] collaboration for joint PhD degree between EMBL and Heidelberg University, Faculty of Biosciences

[3] Masters Course in Biomedical Engineering, Faculty of Civil and Industrial Engineering, Sapienza University, Piazza Aldo Moro 5, 00185 Roma, Italy

* To whom correspondence should be addressed: gross@embl.it,

Abstract

Territorial animals must be able to express social aggression or avoidance in a manner appropriate to spatial context and dominance status. Recent studies indicate that the ventromedial hypothalamus controls both innate aggression and avoidance, suggesting that it may encode an internal state of threat common to both behaviors. Here we used single unit *in vivo* calcium microendoscopy to identify neurons in the mouse ventromedial hypothalamus encoding social threat. Threat neurons were activated during social defeat as well as when the animal performed risk assessment. Unexpectedly, threat neurons were also activate in the chamber where the animal had been previously defeated and a distinct set of neurons emerged that were active in its home chamber, demonstrating the dynamic encoding of spatial context in the hypothalamus. Ensemble analysis of neural activity showed that social defeat induced a change in the encoding of social information and optogenetic activation of ventromedial hypothalamus neurons was able to elicit avoidance after, but not before social defeat, demonstrating a functional reorganization of the pathway by social experience. These findings reveal how instinctive behavior circuits in the hypothalamus dynamically encode spatial and sensory cues to drive adaptive social behaviors.

Introduction

Comparative molecular and functional studies across animal species demonstrate that the hypothalamus contains evolutionarily conserved brain networks for controlling survival behaviors and maintaining physiological homeostasis (Swanson, 2000; Tosches & Arendt, 2013). Work in laboratory rodents has shown that the medial hypothalamus, in particular, harbors distinct neural systems essential for defense and reproduction (Canteras, 2002). The best understood of the medial hypothalamic nuclei is the ventromedial nucleus (VMH) whose dorsal medial (VMHdm) and ventrolateral (VMHvl) divisions are key nodes in the defensive and reproductive systems, respectively (Canteras et al., 1994; Canteras, 2002). VMHdm is required for defensive responses to predators (Silva et al., 2013; Kunwar et al., 2015; Viskaitis et al., 2017), while VMHvl is necessary for mounting and territorial aggression, key reproductive behaviors (Lin et al., 2011; Yang et al., 2013). However, loss of function studies demonstrate that defensive responses to social threats do not depend on VMHdm, but rather require VMHvl, suggesting that the reproductive system plays a more general role in controlling both aggression and defense to social stimuli (Silva et al., 2013; Silva et al., 2016). Consistent with a general role in social threat responding electrical, pharmacogenetic, or optogenetic stimulation of VMHvl is able to elicit or increase the probability of social aggression (Olivier, 1977; Kruk et al., 1983; Lin et al., 2011; Lee et al., 2014; Hashikawa et al., 2017; Yang et al., 2017; Wang et al., 2019) and avoidance (Sakurai et al., 2016; Wang et al., 2019). However, these responses are often unreliable and have been shown to be influenced by the social and hormonal status of both the subject and the threat (Lin et al., 2011; Lee et al., 2014; Sakurai et al., 2016; Yang et al., 2017) suggesting a role for past experience or other environmental factors in dictating the behavioral output of VMHvl.

Neurons in VMHvl show firing patterns that correlate with social investigation and attack (Lin et al., 2011; Falkner et al., 2014; Remedios et al., 2017) and cFos and bulk calcium imaging approaches identified partially overlapping recruitment of neural activity during social aggression and defeat (Motta et al., 2009; Sakurai et al., 2016; Wang et al., 2019). However, single unit recordings have not been reported during social defeat or avoidance and it remains unclear what aspects of these behaviors are encoded in VMHvl and whether the overlap between aggression and defense reflects a common behavioral or internal state component. VMHvl receives major afferents from the medial amygdala that encodes information about conspecific identity (Canteras, 1995; Swanson & Petrovich, 1998; Li et

al., 2017). However, VMH also receives inputs from lateral septum and subiculum that could convey contextual information (Risold & Swanson, 1997; Silva, et al., 2016; Wong et al., 2016; Lo et al., 2019) and both of these input pathways are able to modulate aggression (Wong et al., 2016; Leroy et al., 2018) suggesting that VMHvl is in a position to integrate sensory and spatial information to guide social behavior. Finally, ensemble neural activity elicited in VMHvl during social investigation can be reshaped by sexual experience, demonstrating a capacity for experience-dependent changes in VMHvl (Remedios et al., 2017).

Here we investigated the functional encoding of defense and aggression by VMHvl using single unit neural activity recording and optogenetic manipulation during male-male social encounters in laboratory mice. A majority of neurons in VMHvl were active in a way that was consistent with the encoding of a generalized internal state of threat, responding during a variety of social threat situations. Unexpectedly, following social defeat sets of neurons emerged that were activated by the context where the social threat had occurred or by the home cage where the animal resided, demonstrating the experience-dependent encoding of spatial context. Moreover, social defeat reshaped the neuron ensemble activity elicited during social interaction and optogenetic stimulation could elicit robust escape behavior in defeated animals, but not in undefeated controls. These findings demonstrate that VMHvl dynamically encodes social threat and spatial context states in a manner that can guide defensive behavior.

Results

Encoding of social threat

In order to better understand what aspects of defense are encoded in VMHvl neuron firing, we used *in vivo* microendoscopic calcium imaging to measure neuronal response properties in mice subjected to social defeat (**Figure 1a-e**). Mice were habituated to a home chamber from which they were given access to a corridor and far chamber for a brief period each day. On the social defeat day, mice were closed into the far chamber and an aggressive mouse was introduced. Following social defeat, the far chamber door was opened to allow the mouse to escape and exhibit approach-avoidance behavior toward the aggressor who remained restricted to the far chamber. Many neurons (100/246, 40%, Social+) showed an increase in activity during close social interaction that returned to baseline levels during the subsequent approach-avoidance phase (**Figure 1f-h**). Other neurons (79/246, 32%, Social-)

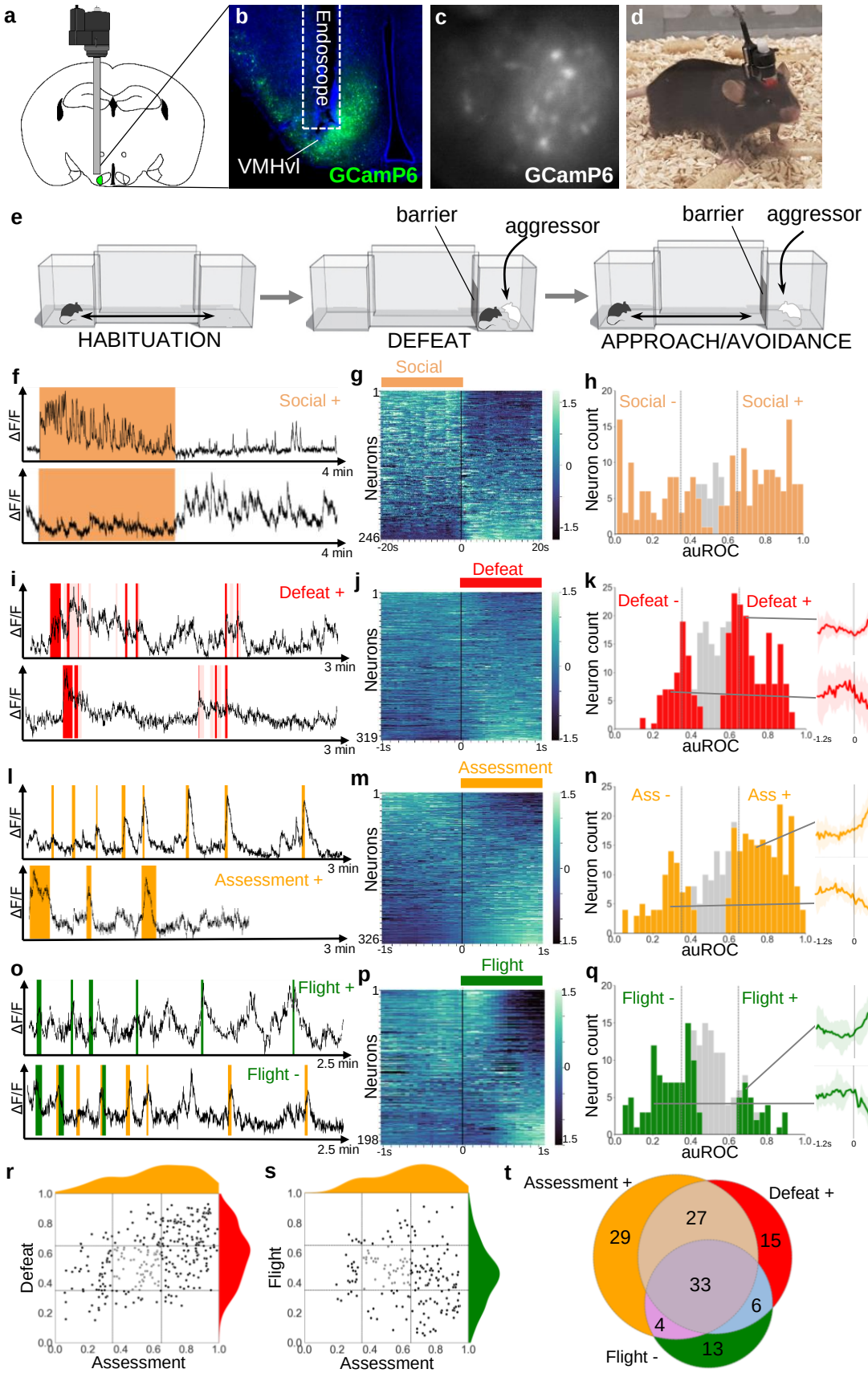

Krzywkowski et al., **Figure 1**

Figure 1. **VMHvl encodes social threat.** (**a-d**) Microendoscopy was used to image single unit calcium activity in VMHvl neurons of awake behaving mice expressing GCaMP6s. (**c**) Representative processed endoscope image used to extract relative changes in fluorescence (ΔF/F) for putative single neurons. (**e, left**) Mice were housed in a home chamber for several days during which time they were given access to a corridor and far chamber for 15 minutes each day. (**e, middle**) On the defeat day the mouse was enclosed into the far chamber and an aggressor was introduced who repeatedly attacked the mouse. (**e, right**) Subsequently, the barrier was opened and the defeated mouse exhibited approach and avoidance behavior toward the far chamber. (**f, i, l, o**) Activity traces of representative neurons showing increased (+) or decreased (-) signal during specific behaviors (color). (**g, j, m, p**) Summary of activity of all neurons across the onset or offset of each behavior. (**h, k, n, q**) Histogram of area under the receiver operator curve (auROC) for all neurons with significantly responding neurons indicated in color and average z-score ± SD (N = 5-12) traces of representative significant positive and negative responding neurons shown at right ($P < 0.05$). Vertical lines in histogram indicate high (0.65) and low (0.35) cut-off for scoring positively responding neurons. (**r, s**) Correlation of neuron auROC scores across behaviors. Distributions are shown outside the axes. (**t**) Overlap of Defeat+, Assessment+, and Flight- neurons (N = 4).

showed the opposite pattern, with unaltered or decreased activity during social investigation and increased activity during the approach-avoidance phase (**Figure 1f-h**). A smaller set of neurons showed changes in activity that were time-locked to individual defeat events (117/319, 36%, Defeat+; 36/319, 11%, Defeat-) when the intruder attacked the experimental animal (**Figure 1i-k**). These findings are consistent with earlier cFos and bulk calcium imaging studies (Motta et al., 2009; Sakurai et al., 2016; Wang et al., 2019) and confirm that VMHvl is strongly recruited during social defeat.

Next, we examined neural activity patterns during the post-defeat, approach-avoidance phase. The mice repeatedly advanced in a cautious manner toward the aggressor, exhibiting frequent risk assessment behaviors in which they stretched their body in the direction of the far chamber (stretch-attend or stretch-approach, Blanchard et al. 2011). Once close to the far chamber mice often turned and fled back to the home chamber (flight, **Video 1**). Calcium imaging identified many cells that were robustly activated during risk assessment either close to or far away from the far chamber (160/326, 49%, Assessment+). Smaller sets of cells were either deactivated during risk assessment (63/326, 19%, Assessment-) or activated or deactivated during flight (30/198, 15%, Flight+; 60/198, 30%, Flight-; **Figure 1l-q**). Notably, Assessment+ cells were activated during risk assessment events that occurred at a distance from the far chamber, particularly at the junction of the home cage and corridor (**Figure 1o**; **Video 2**). A comparison of neuronal response properties revealed that a majority of Assessment+ cells (81/152, 53% vs chance 17%, $P < 0.001$) overlapped with Defeat+ cells, suggesting that they may encode a generalized internal state associated with both direct threat as well as the assessment of threat even when this does not involve close social contact (**Figure 1r**). Moreover, many Assessment+ cells (37/100, 37% vs chance 14%, $P < 0.001$) were also Flight- cells, showing activation as the mouse approached the far chamber and then turning off abruptly when the animal fled (**Figure 1s**; **Video 1**). A similar firing response pattern has been reported for neurons in VMHdm during approach toward a predator (Masferrer et al., 2018). Overall, Defeat+, Assessment+, Flight- cells showed a high degree of overlap (26% vs chance 5%, $P < 0.001$) and made up the largest fraction of responsive neurons (**Figure 1t**). These findings suggest that VMHvl neurons may encode a generalized social threat state rather than particular behaviors associated with threat response.

144 ***Dynamic encoding of spatial context***

145 Our observation that a large fraction of neurons in VMHvl were activated during risk
146 assessment both close and far from the social stimulus could be explained by the multi-
147 sensory inputs that VMHvl receives (Canteras et al., 1995; Garfield et al., 2014; Lo et al.,
148 2019; Wong et al., 2016). In particular, our earlier observation that VMHdm is required for
149 the expression of defensive behaviors in a context previously associated with a predator
150 suggested that the medial hypothalamus can be recruited by stimulus-associated cues (Silva
151 et al., 2016) and is consistent with evidence for activation of VMHvl during nose poke in
152 anticipation of aggression (Falkner et al., 2016). To test for the recruitment of VMHvl by
153 purely contextual cues, we performed *in vivo* calcium endoscopy in animals who
154 experienced social defeat and were re-exposed 24 hours later to the defeat context in the
155 absence of the aggressor (**Figure 2a**). Analysis of neuronal response properties revealed a
156 large fraction of neurons with robust activation in the defeat chamber (93/343, 27%, Far
157 chamber+, **Figure 2b-d**). Unexpectedly, a second group of neurons showed marked
158 activation in the home chamber (78/343, 23%, Home+, **Figure 2e-g**). Notably, Home+ and
159 Far chamber+ cells abruptly turned off when the animal passed from the chamber to the
160 corridor, suggesting that they specifically responded to the far and home chamber contexts,
161 rather than to a gradient of social threat cues, for example. A comparison of neuronal
162 response properties between the context, approach-avoidance, and defeat phases of the test
163 showed that Far chamber+ neurons strongly overlapped with Social+ neurons (45/67, 67%
164 vs chance 11%, $P < 0.001$) and Home+ neurons with Social- neurons (37/60, 62% vs chance
165 7%, $P < 0.001$; **Figure 2ij**) and that Far chamber+ neurons also overlapped with Defeat+
166 neurons (35/84, 42% vs chance 10%, $P < 0.001$; **Figure 2k**) and, in a three way comparison,
167 a larger fraction of Far chamber+ than Home+ neurons were Assessment+ or Defeat+
168 (**Figure 2l,o**). These data suggest that VMHvl encodes a generalized state of social threat
169 that can be reactivated by contextual cues (Social+, Defeat+, Far chamber+) as well as
170 features of social territory (Home+).

171 To understand whether the recruitment by context was linked to the past experience of the
172 animal we compared context encoding in animals before and after social defeat. Only a
173 small number of Far chamber+ and Home+ cells could be identified during the pre-defeat
174 habituation phase even though the animal explored the apparatus to a similar extend in both
175 phases (**Figure S3**). To quantify changes in neuron activity before and after defeat we
176 employed linear discriminant analysis (LDA) of neuron ensemble activity. Before defeat,

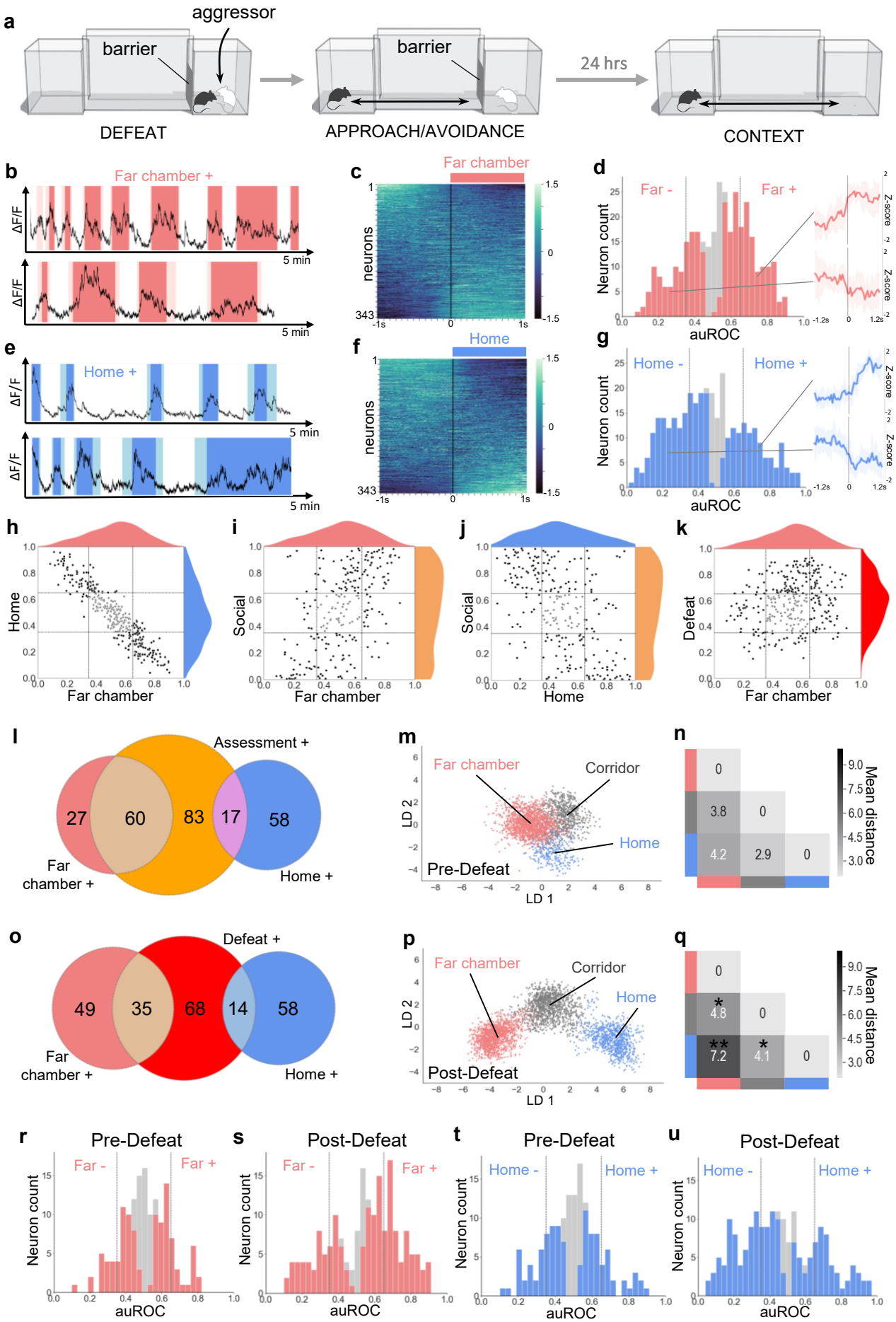

Krzywkowski et al., **Figure 2**

Figure 2. **Dynamic encoding of spatial context in VMHvl.** (**a**) *In vivo* calcium endoscopy was carried out in mice subjected to (**left, middle**) social defeat and then exposed again to (**right**) the defeat context one day later. (**b, e**) Activity traces of representative neurons showing increased (+) signal when the mouse enters the far or home chamber (dark color) or its immediately adjacent corridor (light color). (**c, f**) Summary of activity of all neurons across the transition into the far or home chamber. (**d, g**) Histogram of area under the receiver operator curve for all neurons with significantly responding neurons indicated in color and average z-score traces ± SD (N = 9-10) of representative significant positive and negative responding neurons shown at right ($P < 0.05$). Vertical lines in histogram indicate high (0.65) and low (0.35) cut-off for scoring positively responding neurons. (**h-k**) Correlation of neuron auROC scores between chambers and/or behavior. Distributions are shown outside the axes. (**l, o**) Overlap of Far chamber+, Home+, Assessment+, and Defeat+ neurons (N = 7). (**m, p**) LDA plot of neuron ensemble activity for a representative mouse in the home, far chamber, or corridor. Each data point represents a frame of calcium imaging data projected onto the first two linear discriminants. (**n, q**) Average distances between clusters of frames representing neuron ensemble activity for all mice (*$P < 0.05$, **$P < 0.01$). (**r-u**) Histograms of area under the receiver operator curve for all neurons with significantly responding neurons indicated in color. Vertical lines indicate high (0.65) and low (0.35) cut-off for scoring positively responding neurons. (**m, n, r, t**) Habituation phase before social defeat, and (**p, q, s, u**) context phase after social defeat (N = 4).

neuron ensemble activity in the home, corridor, and far chambers was overlapping as visualized using principal LDA discriminants (**Figure 2mn** and **Figure S1**). Following defeat, however, home, corridor, and far chamber ensemble activity became significantly more separated (**Figure 2pq** and **Figure S2** Home vs. Far chamber LDA distance, $P < 0.01$) confirming the observation that social defeat induced a marked enhancement of the encoding of spatial context and suggesting that VMHvl may dynamically encode features of territory.

Overlapping encoding of aggression and defense

Having established that VMHvl encodes features of social threat and context we examined the hypothesis that social threat neurons would also be active during aggression. First, we performed serial cFos labeling using TRAP-tagging (*cFos*::CreERT2; *Rosa26*::LSL-tomato; Guenthner et al., 2013) to determine the extent of overlap in recruitment during social defeat and resident-intruder aggression. Naïve animals were subjected to two resident-intruder tests at one week interval in which they were either the resident or intruder, in all possible combinations (Aggression-Aggression, Defense-Defense, Aggression-Defense, Defense-Aggression). Immediately following the first test mice were treated with 4-OHT to induce persistent labeling of cFos+ cells, followed by immunolabeling of cFos+ cells after the second test. Animals subjected to the same behavioral experience (Aggression-Aggression or Defense-Defense) showed 50±15% overlap of cFos+ cells while those with different experiences (Aggression-Defense or Defense-Aggression) showed 18±5% overlap and those under control conditions 10±2% overlap (ANOVA: $F = 20.89$, $P = 0.0001$; **Figure 3a-d**). These data are consistent with experiments using a viral cFos-tagging strategy (Sakurai et al., 2016) and suggest that approximately one quarter of the cells in VMHvl activated during aggression and defense are recruited by both experiences and that this population of cells may support a common function during male-male social interaction.

Next, we used *in vivo* calcium endoscopy to understand whether VMHvl neurons recruited during aggression might overlap with the social threat and context neurons identified following defeat. Robust aggression was elicited by confining the mouse to its home cage and introducing a subordinate male mouse. During aggression phasic modulation of neuron activity occurred during bouts in which the resident actively investigated (56/310, 18% Sniff+; **Figure 3e-g**) or attacked (38/266, 14% Attack+; **Figure 3h-j**) the intruder. Comparison of neuronal response properties revealed that most Attack+ neurons (19/37, 51% vs chance 3%, $P<0.001$) were Sniff+ neurons (**Figure 3k**), consistent with a strong

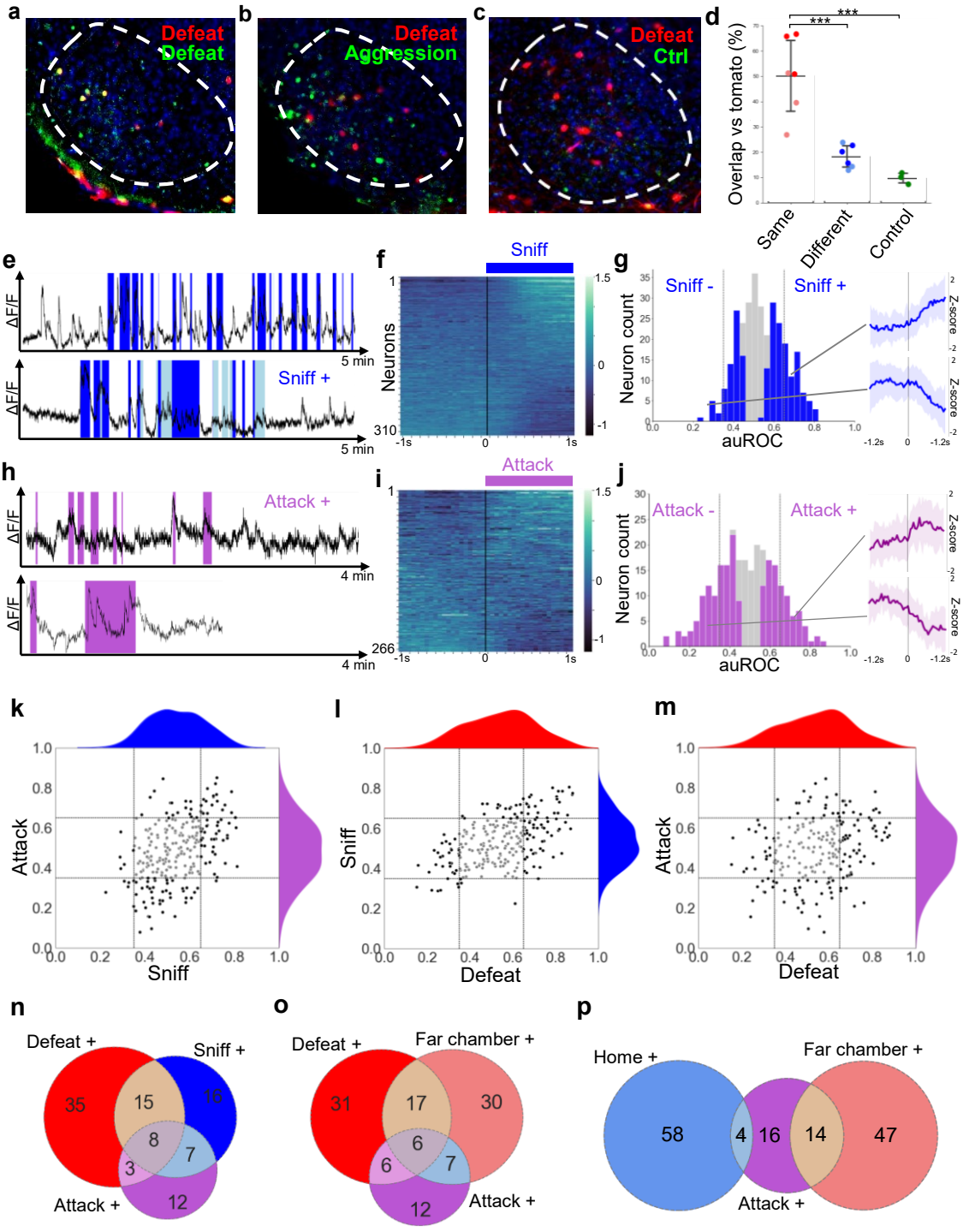

Krzywkowski et al., **Figure 3**

Figure 3. **Overlapping encoding of social defense and aggression.** (**a-c**) Representative images of cFos-tagged (red) and cFos-immunolabeled (green), and double labelled (yellow) cells in brain sections from mice subjected sequentially to social defeat and aggression in a counterbalanced manner. (**d**) Average percentage overlap of defeat and aggression recruited cFos+ cells as revealed by the difference between cFos+ overlap for same, different, or control behaviors (dark red: Defeat-Defeat, dark blue: Defeat-Aggression, green: Defeat-Control; light red: Aggression-Aggression, light blue: Aggression-Defeat; Same vs. Different, $P < 0.001$ N = 6; Same vs. Control, $P < 0.001$, N = 3-6; Different vs. Control, $P > 0.05$, N = 3-6; bars represent SD). (**e, h**) Activity traces of representative neurons showing increased (+) signal during close social investigation (Sniff+, dark blue; ano-genital sniffing, light blue) and aggression (Attack+). (**f, i**) Summary of activity of all neurons across the onset of behavior. (**g, j**) Histogram of area under the receiver operator curve for all neurons with significantly responding neurons indicated in color and average z-score traces ± SD (N = 22-34) of representative significant positive and negative responding neurons shown at right ($P < 0.05$). Vertical lines in histogram indicate high (0.65) and low (0.35) cut-off for scoring positively responding neurons. (**k-m**) Correlation of neuron auROC scores among aggression behaviors and between aggression and defense behaviors. Distributions are shown outside the axes. (**n-p**) Overlap of aggression, defense, and territory-related neurons (N = 5).

overlap between these populations in previous single unit recording studies (Lin et al., 2011; Falkner et al., 2014). Comparison of neuronal response properties across social defeat and aggression showed that a large fraction of Defeat+ neurons (24/68, 35% vs chance 6%, P<0.001) were reactivated during active investigation of the subordinate (Sniff+), indicating that these may encode a common social threat state in both defenders and attackers (**Figure 3l**). A smaller fraction of Defeat+ neurons (12/60, 20% vs chance 5%, P<0.05) were Attack+ neurons (**Figure 3m**) and a three way comparison revealed that 42% of Defeat+ cells overlap with either Sniff+ or Attack+ (**Figure 3n**), a finding that is consistent with our cFos data (**Figure 3a-d**) and confirms the recruitment of both common and unique neuron ensembles during defense and aggression. Comparison of aggression responsive neurons with those activated by the defeat context (Far chamber+) revealed an overlap between Attack+, Defeat+, and Far chamber+ neurons (**Figure 3o**). Unexpectedly, Attack+ neurons showed more overlap with Far chamber+ (14/34, 41% vs chance 4%, P<0.001) than Home+ neurons (4/34, 12% vs chance 3%, P=0.356; **Figure 3p**) despite the fact that the attack occurred in the home cage, reinforcing the idea that aggression elicits features of social threat, rather than safety.

Social defeat remodels neural activity and function

Following on our observation that social defeat elicited changes in contextual encoding in VMHvl (**Figure 2**) and previous experiments showing that sexual experience can remodel VMHvl ensemble activity elicited by exposure to a social stimulus (Remedios et al., 2017) we investigated the possibility that social defeat might also induce changes in neural activity elicited during social encounter. Animals were exposed to repeated social defeat experiences in the far chamber of a dual chamber apparatus as described earlier (**Figure 1e**). The experimental animals showed similar frequencies of behaviors across the two days of social defeat (**Figure S4**). Nevertheless, we restricted our ensemble analysis to data extracted from bouts of close social encounter (defeat, upright, orientating, sniffing, following, see **Materials & Methods**), so as to minimize any confounding effect of potential changes in behavior across experimental sessions. Linear discriminant analysis (LDA) was used to track and quantify shifts in neuron ensemble encoding across sessions. Neuron ensemble activity elicited during the first and second social defeat experiences were significantly non-overlapping (**Figure 4ab** and **Figure S6**). As a control, we used LDA to track and quantify neuron ensemble activity across sessions of resident-intruder aggression carried out as previously described (**FigureS5**). Unlike social defeat and consistent with previous studies

(Remedios et al., 2017) repeated aggression was not associated with changes in neuron ensemble activity (**Figure 4ab** and **Figure S6**) demonstrating that defeat has a unique capacity to alter the encoding of social cues in VMHvl. Notably, this change was found only when defeats preceded, but not when they followed aggression experiences (**Figure S7**). This finding demonstrates that changes in neuron ensemble encoding seen across days are likely due to experience-dependent plasticity rather than spontaneous fluctuations in firing patterns, and suggests that repeated exposure to aggression and winning may impart resistance to the transforming effects of social defeat on social encoding in VMHvl.

Changes in neuron ensemble encoding in VMHvl following social defeat could reflect plasticity in upstream brain regions that provide afferent inputs to VMHvl or they could be due to plasticity within VMHvl. To distinguish these possibilities we used a gain-of-function approach. Previous work showed that optogenetic activation of estrogen receptor α expressing (Esr1+) neurons in VMHvl can elicit aggression against females or castrated males (Lee et al., 2014; Wang et al., 2019). Notably, however, in some cases such animals showed brief avoidance responses during the initial stimulation trials (Lee et al., 2014) suggesting that VMHvl Esr1+ neurons are capable of promoting both aggression and avoidance, possibly in a way that depends on context, dominance status, or social experience. To test whether social defeat might induce changes in VMHvl Esr1+ function we expressed the blue light-activated cationic channel, channelrhodopsin 2 (ChR2), in Esr1+ VMHvl neurons (AAV-*Ef1α*::FLEX-ChR2, *Esr1*::Cre mice) and subjected the animals to two sessions of social defeat (**Figure 4c-e**).

Several hours after social defeat a subordinate intruder mouse was introduced into the home cage of the animal and following a period of habituation, light pulses were delivered to activate Esr1+ neurons. Following social defeat optogenetic activation of Esr1+ neurons elicited rapid and robust defensive behaviors, including freezing, flight, a reduction in social interaction, and immobility in all animals (**Figure 4f**). In one particularly striking case, optogenetic activation of Esr1+ neurons occurring while the resident was attacking the intruder caused an abrupt cessation of aggression and evoked sudden flights away from the subordinate animal (**Video 3**). Notably, no significant increase in defensive behavior was elicited by optogenetic activation in ChR2-expressing mice that were stimulated during a resident-intruder test on the day before the social defeat (**Figure 4g**), nor in mice expressing a control virus (AAV-*Ef1α*::FLEX-YFP, *Esr1*::Cre). These data demonstrate that VMHvl

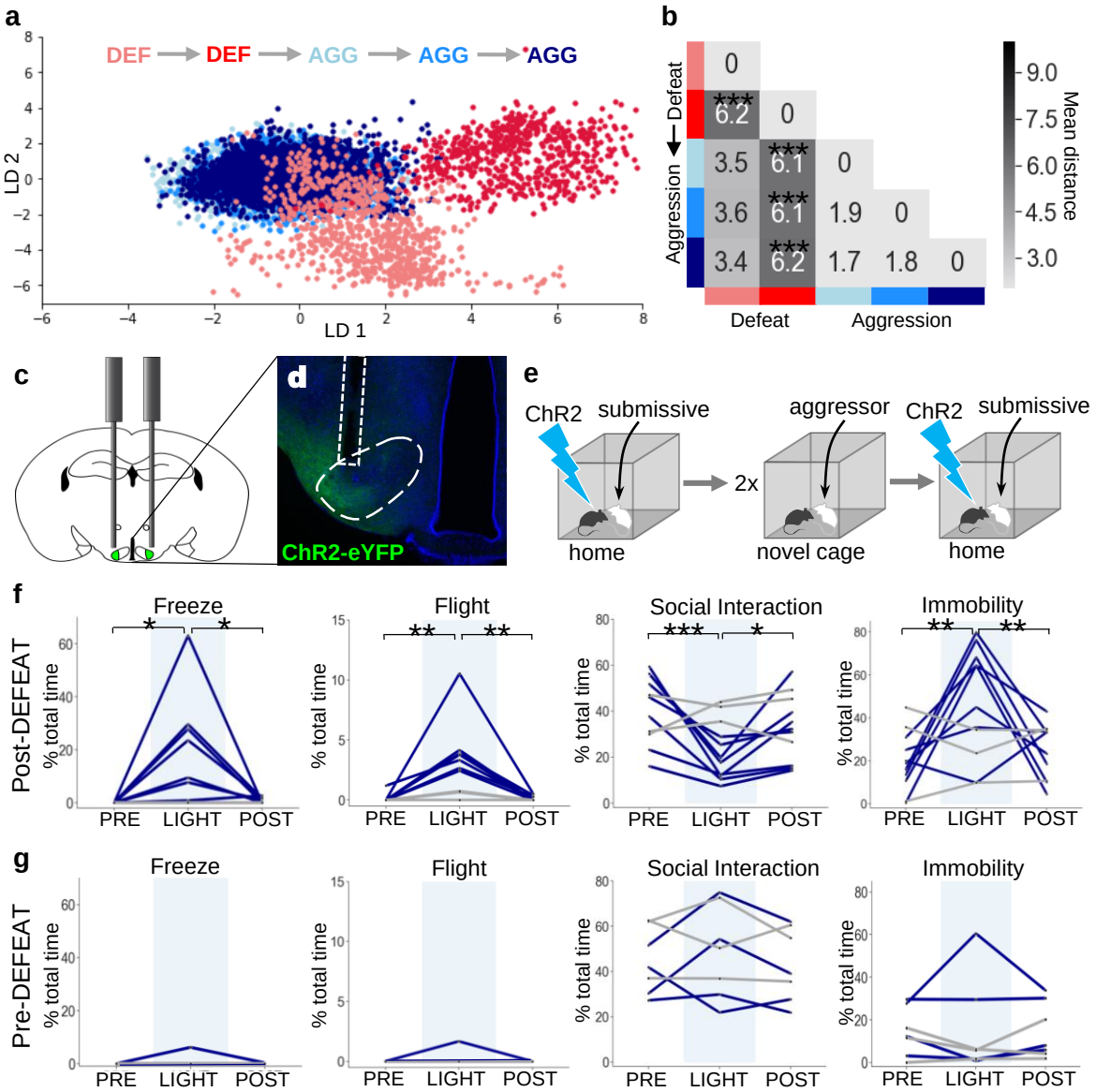

Krzywkowski et al., **Figure 4**

Figure 4. **Social defeat remodels VMHvl activity and function.** (**a**) LDA plot of neuron ensemble activity for a representative mouse during repeated defeat and aggression episodes. Each data point represents a frame of calcium imaging data projected onto the first two linear discriminants. (**b**) Average distances between clusters of neuron ensemble data between defeat and aggression episodes for all mice during forward order testing (N = 4; colors refer to episodes in **a;** *P < 0.05, **P < 0.01, ***P < 0.001) colors refer to episodes in **a**). (**c-d**) Optogenetic stimulation of Esr1+ neurons following local delivery of AAV-*Ef1a*::FLEX-ChR2-eYFP into the VMHvl of *Esr1*::Cre mice. (**e**) Mice were stimulated intermittently (20 Hz, 20 ms pulse, 30 s ON) following the introduction of a subordinate mouse into the home cage before (Pre-Defeat) and/or after (Post-Defeat) two episodes of social defeat in the far chamber. (**f-g**) Trial-averaged (N = 4-5 trials) behavioral measures before (Pre, 30 s), during (Light, 30 s), and after (Post, 30 s) optogenetic stimulation of Esr1+ neurons in VMHvl during either the (**f**) Post-Defeat or (**g**) Pre-Defeat episodes (N = 3-7, *P < 0.05, **P < 0.01, ***P < 0.001).

neurons promote aggression and defense in a manner that depends on social experience and argue that at least part of the plasticity in neuron ensemble recruitment during social interaction (**Figure 4ab**) occurs within or downstream of VMHvl.

Discussion

By performing single unit *in vivo* recordings during social defeat as well as during the post-defeat approach-avoidance period, again during re-exposure to the threat context one day later, and during resident-intruder aggression we were able to examine the encoding of social threat in the VMHvl across a wide variety of defensive behaviors. Neurons activated when the animal was attacked were reactivated later when the animal performed risk assessment behaviors (**Figure 1l,o; Video 2**) and many of them were reactivated when the animal explored the chamber where the defeat occurred one day later (**Figure 2l,o**). Moreover, a significant fraction of social threat cells were activated when the same mouse sniffed or attacked a subordinate mouse in its home cage (resident-intruder test, **Figure 3n**) consistent with the view that conspecific aggression in mice is driven by a defensive instinct aimed at expelling competitors from their territory and ensuring access to reproductive and nutritional resources (Lorenz, 1963) Nevertheless, overall, neurons were more robustly activated when the animal was being attacked then when they were attacking, suggesting a more efficient recruitment of VMHvl by threat in the losing animal (**Figure 1i-n** and **Figure 3h-j, n**). These data allow us to conclude that a major function of VMHvl is to provide an internal state of social threat that can be generalized across a wide variety of defensive behaviors and cues.

Our observation that social defeat drove the rapid emergence of a unique set of cells that fired in the home chamber and did not overlap with those encoding social threat (**Figure 2h-i, o-q**) was unexpected and shows that VMHvl encodes aspects of spatial context beyond those associated with threat. Although the function of these home cells is presently unknown, we speculate that they encode aspects of the animal's territory and that they may function to support territorial behaviors such as scent marking, sex, and defensive aggression. We noted that Home+ and Far chamber+ cells were modulated abruptly when the animal entered or exited the relevant chamber, suggesting that they encode context rather than a gradient of threat (**Figure 2b,e**). VMHvl receives inputs from the ventral hippocampus via LS that could contribute territory-related contextual information (Risold et al., 1997; Strange et al., 2014) and are able to modulate conspecific aggression in VMHvl

(Leroy et al., 2018; Wong et al., 2016). Our findings open up the possibility that contextual and social cues are integrated in a dynamic manner in VMHvl to drive and modulate a wide variety of behaviors aimed at territorial defense.

Our neuron ensemble analysis shows that social defeat reshaped both spatial context as well as social cue encoding. Ensemble neuron activity elicited during close social investigation became transformed following a social defeat experience, but not following a social aggression experience (**Figure 4a-b**). The latter observation is consistent with a previous recording study in which resident-intruder aggression failed to induce changes in VMHvl ensemble activity, while sex did (Remedios et al., 2017). Finally, our gain-of-function experiment demonstrates that the social defeat-induced transformation of encoding involves functional plasticity in or downstream of VMHvl Esr1+ neurons (**Figure 4c-g**). We note that in our hands optogenetic stimulation of VMHvl Esr1+ neurons was unable to elicit reliable aggression behavior against intact male intruders under baseline conditions, a finding that is consistent with previous studies where such stimulation only elicited reliably aggression against females or castrated males and in which a significant fraction of animals showed brief avoidance behavior upon initial optogenetic stimulation (Lee et al., 2014; Lin et al., 2011). We interpret these findings to indicate that VMHvl is primed to promote either defensive avoidance or defensive aggression under baseline conditions in a manner that depends on past social experience. This interpretation is supported by a study showing that pharmacogenetic activation of progesterone receptor expressing neurons in VMHvl can increase the reliability of attack in the resident-intruder assay if the animal was previously singly housed, but not if it was group housed (Yang et al., 2017).

Our observations reveal the encoding and control of instinctive motivational states by VMHvl neurons, showing that these encode an experience-dependent map of spatial context and that they exhibit functional plasticity in response to past social experience that guides the selection of instinctive behavioral outputs. These data argue for a reevaluation of the role of the hypothalamus in behavior. Rather than being viewed as a hardwired, innate behavioral response region, it should be seen as an integrator of present and past sensory and contextual information that adapts survival behaviors to a changing environment.

Materials & Methods

Animals and behavioral apparatus

All experimental procedures involving the use of animals were carried out in accordance with EU Directive 2010/63/EU and under approval of the EMBL Animal Use Committee and Italian Ministry of Health License 541/2015-PR to C.G. Animals were maintained in a temperature and humidity controlled environment with food and water provided *ad libitum* and 12h/12h light-dark cycle with lights on at 7:00. Experimental male C57BL/6J wild type (Charles River) and *Esr1*::Cre (Stock No. 017913, Jackson Laboratory) mice were switched to reverse dark-light cycle (lights off at 9:00) and singly housed in the home cage of the behavioral apparatus at least one week before initiating the experimental procedures and tested during the dark period under red lighting (two 1W LED lights). The custom Plexiglas behavioral apparatus consisted of three detachable parts: 1) home cage with dimensions 25x25x25 cm with a Y-shaped slit, 4 cm wide at the bottom serving as an entrance closed by sliding doors, 2) stimulus chamber identical to home cage, and 3) a corridor 46x12x30 cm connecting home cage and stimulus chamber (modified from Silva et al., 2013). Aggressor mice were CD-1 adult retired breeders (Charles River) screened for robust aggression and singly housed (Franklin et al., 2017). Subordinate mice were 9-15 week old BALB/c males bred at EMBL. Mice cages were changed weekly.

Surgical procedures

Mice were anesthetised before surgery with 3% isoflurane (Provet) in oxygen and placed in stereotaxic frame (Kopf). Anaesthesia was maintained with continuous 1-2% isoflurane administration in breathing air enriched with oxygen. Body temperature was maintained with a heating pad. During surgery the skull was exposed, aligned, and cleaned with 0.3% hydrogen peroxide solution. For optogenetic activation experiments 0.1-0.2 µl of AAV5-*Ef1a*::DIO-hChR2(E123T/T159C)-EYFP or AAV5-*Ef1a*::DIO-EYFP virus (UNC Vector Core) was infused bilaterally into VMHvl (from Bregma L:+/-0.67, A/P: -0.98, D/V: -5,75). After 5-10 min the glass capillary was retracted and custom-made optic fibre connectors were implanted (0.66 NA, 200 µm core fibre and ceramic ferule with 230 µm /1250 µm internal/external diameter; from Bregma L: +/-0.67, A/P: -0.98, D/V: -5.55 and L: +/-1.14, A/P: -0.98, D/V: -5.6, at 5° angle). For *in vivo* calcium endoscopy 0.2-0.3 µl of AAV5-*hSyn*::GCaMP6s (Penn Vector Core) virus was injected unilaterally into VMHvl and the endoscope lens (Snap-imaging cannula model L type E, Doric Lenses) was implanted at a

very slow rate (from Bregma L: +/-0.67, A/P: -0.98, D/V: -5.7). All implants were secured to the skull using miniature screws (RWD) and dental cement (Duralay). The wound was cleaned and skin was stitched around the implant. After the surgery mice received intra-peritoneal injection of 0.4 ml saline and were placed into heated cages with drinking water containing paracetamol for ~1 week. Mice were maintained in isolation for ~4 weeks before experimentation.

Social defeat test

On the social defeat day, the mouse was allowed to explore the apparatus freely for 5 minutes, after which the animal was closed in the stimulus chamber and an aggressor was introduced for 10 minutes. In a few cases the animal was allowed to escape earlier to avoid excessive defeat. The mouse was released from the stimulus chamber and the door closed to confine the aggressor to the stimulus chamber. After social defeat the mouse was allowed to explore the apparatus freely for at least 5 minutes. The memory test was conducted on the day following after social defeat, during which the mouse could explore the apparatus freely. The apparatus was washed with detergent and 50% alcohol between mice to avoid any remaining smell that could influence behavior of the test subject. CD-1 aggressors were screened for aggression for 3 days. Every day an intruder was placed in the aggressor's cage for 3 minutes. Only mice that attacked the intruder on every occasion were selected.

Aggression test

On the aggression day a BALB/c intruder was introduced for 10 min after which the intruder was removed. BALB/c intruders used for this test were 9-15 weeks old and housed 3-5 mice per cage. For cFos experiments animal were allowed to explore the entire apparatus for 5 min before and after introduction of the intruder in order to match exploration in the social defeat test.

Behavioral data acquisition and annotation

Behavior was recorded at 40-50 Hz from above with up to two cameras (acA1300-60gmHIR, Basler) with GigE connections using Pylon software. Frame-by-frame behavioral annotation was carried out manually using Observer XT11 (Noldus) and Solomon Coder software. The experimenter was blind to genotype or calcium trace of recorded neurons when scoring behavior. The following behaviors were scored: defeat – biting attack toward the experimental animal in which the animal exhibited avoidance behavior (whole body

movement away from intruder); *assessment* – stretch attend or stretch approach behavior in which the animal extended its body in the direction of the threat or threat chamber from an immobile or slowly moving position; *flight* – rapid movement away from the threat or threat chamber; attack – biting attack or vigorous anogenital sniffing toward the intruder animal; *sniffing* – close contact of the nose of the experimental animal with the intruder; upright – animal rises on back paws with head up, keeping front paws stretch out ; put down – keeping other animal down usually with two front paws and staying on top of it; follow – experimental animal closely follows intruder; cornering – staying in the corner of the apparatus (animal has body contact with two walls); locomotion – free movement and exploration of experimental apparatus; freeze – no body movement ; head/body orientation – turning head or whole body towards another conspecific. Any animals with misplaced viral infections or optic fiber implants were excluded from the analysis.

Histology

All animals were deeply anesthetized and transcardially perfused with PBS (Invitrogen) followed by 4% PFA (Sigma) in 0.1M PB solution and then post-fixed in 4% PFA at 4°C for 24h and cut using a vibratome (Leica VT 1000s) in PBS (80µm) for injection or implant location check, or staining (50 µm) procedure. If not used immediately, sections were stored in PBS with 0.1% sodium azide. For anti-cFos staining (SC-52G, Lot FO215, Santa Cruz) sections were washed three times in PBS for 10 min, blocked with 10% normal donkey serum, 0.2% Triton-X in PBS for at least 1h, and incubated with primary antibody (1:500) containing 5% normal donkey serum, 0.2% Triton-X overnight at 4°C. Sections were washed three times in PBS, incubated with secondary antibody solution (1:1000) containing 10% normal donkey serum for 2h at room temperature, washed twice with PBS, and stained with DAPI for 15 min, before washing twice with PBS and mounting on SuperFrost Plus slides (ThermoFischer) with Moviol.

cFos mapping

Double heterozygous *cFos*::CreERT2;*RC*::LSL-tdTomato mice (Stock No. 021882 and 007914, Jackson Laboratory) were isolated for 7 days and subjected to 3 days of habituation to the apparatus before social defeat. A single dose (50mg/kg) of 4-hydroxytamoxifen (4-OHT, 70% z-isomer, Sigma) was injected intra-peritoneally <2 min after social defeat to induce fluorophore expression in neurons recruited by defeat. One week later, mice were again habituated for 3 days to the apparatus and subjected to social aggression, and 1.5h

later trans-cardially perfused and processed for cFos immunofluorescence. In a second group the order of social defeat and social aggression were swapped to produce five experimental groups: defense-defense (same), aggression-aggression (same), defense-aggression (different), aggression-defense (different), defense-control (control). Control indicates mice exposed only to context prior to labelling.

Optogenetic experiments

Heterozygous *Esr1*::Cre mice were injected with virus and allowed to recover for 2-3 weeks, housed under reverse light-cycle for 2 weeks, and then handled and habituated to the optical cables for at least 2 days prior to testing. Initially, after a 2 min free exploration period, each animal was stimulated with light (30 s, 20 Hz) every 1-2 min with increasing power (0.5, 1, 3, 6, 10 mW) to identify the optimal intensity to elicit a behavioral response (immobility or locomotion) and this was subsequently used for further stimulation. Control animals received 6 mW stimulation. For stimulation in the presence of a subordinate intruder free exploration was allowed for ~3 min during which a single light stimulus was delivered (30s, 20Hz) after which a BALB/c intruder was introduced and the animal was further stimulated (3-5 times, 30s, 20Hz) during periods of social interaction. Mice were then subjected to two days of social defeat (5 min) by a CD-1intruder in a novel plexiglas cage following 1 min free exploration. Several hours later, stimulation in the presence of a subordinate intruder was repeated as above. Optical stimulation of ChR2 was achieved using a 465 nm LED (Plexbright, Plexon) attached to a manual rotatory joint with 1m patch cables (Plexbright High Performance, Plexon). Power at the end of the patch cables was measured before each experiment with a portable optical power meter (Thor Labs) and stimulation trains were generated using V2.2 Radiant software (Plexon). Animals with mistargeted viral injections or optic fibers were excluded from the analysis.

Calcium endoscopy

Following GCaMP6 virus infection, GRIN lens imaging canulae (Model L, Doric Lenses) were stereotaxically implanted over the VMHvl and mice allowed to recover for 2-3 weeks followed by 2 weeks isolation under reverse light-cycle and at least 3 days habituation to the microscope plugging and unplugging procedure. Mice were then habituated to the behavioral apparatus for three days, and for the second and third days the microscope body was attached. The following week mice (N = 4) were subjected to two consecutive social defeats tests (day 1: social defeat, day 2: memory) over four days, and 2-3 days later, three

consecutive aggression tests over three days. In a second group of mice (N = 3) the testing order as reversed. Recordings were done with 15-25% LED intensity using 50 ms or 100 ms exposure times. Calcium imaging data was successfully collected from 15/24 animals that underwent surgery. Animals with mistargeted endoscope placements, very few (<15) recorded neurons, recordings exhibiting excessive movement artifacts, or who showed insufficient instances of relevant behaviors were excluded from the analysis (7/15).

Calcium imaging analysis

Image processing was done using Fiji software. Briefly, videos were first loaded as a stack of images in .tiff format. The stack was duplicated and for each frame a background frame was generated using a band pass filter (lower band: 100, higher band: 10,000). Next, each frame of the recording was divided by the corresponding background frame and the resulting background-filtered stack was aligned using TurboReg via the translation batch algorithm. Neuronal ROIs were manually selected from the maximum intensity projection image, with detection aided by inspecting recordings at increased speed to discern dim neurons with slow dynamics. Finally, the mean intensity ROI traces were extracted and $\Delta F/F$ was calculated where F is the mean intensity over the entire recording period. To track ROIs over different recordings and days, an ROI mask was projected onto each new recording and translated if necessary to account for possible field of view movement between recordings. ROIs that could not be assigned to the mask were treated as new ROIs.

Data analysis

For the analysis of neuronal response properties, receiver operating characteristic (ROC) curves were calculated using custom Python scripts (scikit-learn). Briefly, all frames in a selected calcium imaging recording were scored as either positive of negative for a particular behavior and a ROC curve was generated for each neuron by plotting the true positive and false positive rates across the distribution. The area under the ROC curve (auROC) was calculated for each recording and averaged across days to give a measure of the responsiveness of a neuron to a given behavior. Neurons with auROC values greater than 0.65 or less than 0.35 were considered to respond to the behavior (e.g. Assessment+, Defeat-). Significance of neuronal response auROC values was estimated by calculating the mean and standard deviation (SD) of the distribution of auROC values obtained by shuffling true and false positive labels 1000 times. Neuronal response auROC values $\geq$ 3 SD away from the mean we considered significant. For the analysis of auROC values for flight behavior 2

seconds before and after the initiation of each flight were labeled as true negative and true positive, respectively. Only recordings with at least 2 instances of relevant behavior were selected for auROC analysis. Heat maps were generated by extracting calcium imaging data (meaned z-score over all trials) for individual neurons from before and after the onset or offset of a given behavior. Significant change across behavioral onset or offset was estimated for each neuron by performing a Wilcoxon signed rank-sum test (Python, scikit-learn) on the distribution of values that resulted from averaging the z-scores of frames from the before and after periods for each trial. For linear discriminant analysis (LDA algorithm, Python, scikit-learn) data was normalized within days by calculating z-scores for each recording separately. Each frame was then expressed as a vector containing calcium values for all neurons. The distance between clusters was quantified by calculating the average distance between data points of a given cluster and all other data points from other clusters. For Venn diagrams we included only neurons responding to a behaviors (e.g. Defeat+) that were recorded across all relevant behaviors, resulting in different numbers of neurons across Venn analyses (**Table S1**). Probability of chance overlap was computed by multiplying the probabilities of responsive neurons. Significance was assessed using Fisher's test.

Statistical analysis

Prism Graphpad 5 software or custom scripts in Python were used to generate graphs and perform statistical analysis. For calcium imaging Wilcoxon rank-sum test (Python, scikit-learn package) was performed. For cFos experiments one-way ANOVA with Tukey's post-hoc test was used. For optogenetic experiments repeated measures ANOVA with Tukey's post-hoc test was used. For assessing significance of overlap between different populations of neurons Fisher's test was used. For assessing significance differences in LDA representations the one-way ANOVA and T test were used.

Data and code availability

Custom code written for this study as well as behavioral and imaging data will be made available upon reasonable request.

Author contributions

All behavioral experiments and data analysis were carried out by P.K. B.P. and P.K. carried out the analysis of neuron ensembles. C.T.G. supervised the work and together with P.K. conceived the project, designed the experiments, and wrote the manuscript.

Acknowledgements

We thank Dominic Evans and Tiago Branco for sharing expertise in calcium endoscopy and Daniel Rossier, Irene Ayuso, Senthil Deivasigamani, Hiroki Asari and Santiago Rompani for helpful comments on the manuscript. The work was supported by EMBL and the European Research Council (ERC) Advanced Grant COREFEAR to C.T.G.

References

Blanchard, D. C., Griebel, G., Pobbe, R., & Blanchard, R. J. (2011). Risk assessment as an evolved threat detection and analysis process. *Neuroscience and Biobehavioral Reviews*, *35*(4), 991–998. https://doi.org/10.1016/j.neubiorev.2010.10.016

Canteras, N. S. (2002). The medial hypothalamic defensive system: Hodological organization and functional implications. *Pharmacology Biochemistry and Behavior*. https://doi.org/10.1016/S0091-3057(01)00685-2

Canteras, N. S., Simerly, R. B., & Swanson, L. W. (1994). Organization of projections from the ventromedial nucleus of the hypothalamus: A Phaseolus vulgaris-Leucoagglutinin study in the rat. *Journal of Comparative Neurology*. https://doi.org/10.1002/cne.903480103

Canteras, N. S., Simerly, R. B., & Swanson, L. W. (1995). Organization of projections from the medial nucleus of the amygdala: A PHAL study in the rat. *Journal of Comparative Neurology*. https://doi.org/10.1002/cne.903600203

Falkner, A. L., Dollar, P., Perona, P., Anderson, D. J., & Lin, D. (2014). Decoding ventromedial hypothalamic neural activity during male mouse aggression. *The Journal of Neuroscience : The Official Journal of the Society for Neuroscience*, *34*(17), 5971–5984. https://doi.org/10.1523/JNEUROSCI.5109-13.2014

Falkner, A. L., Grosenick, L., Davidson, T. J., Deisseroth, K., & Lin, D. (2016). Hypothalamic control of male aggression-seeking behavior. *Nature Neuroscience*, *19*(4), 596–604. https://doi.org/10.1038/nn.4264

Garfield, A. S., Shah, B. P., Madara, J. C., Burke, L. K., Patterson, C. M., Flak, J., … Heisler, L. K. (2014). A parabrachial-hypothalamic cholecystokinin neurocircuit controls counterregulatory responses to hypoglycemia. *Cell Metabolism*, *20*(6), 1030–1037. https://doi.org/10.1016/j.cmet.2014.11.006

Guenthner, C. J., Miyamichi, K., Yang, H. H., Heller, H. C., & Luo, L. (2013). Permanent genetic access to transiently active neurons via TRAP: targeted recombination in active populations. *Neuron*, *78*(5), 773–784. https://doi.org/10.1016/j.neuron.2013.03.025

Hashikawa, K., Hashikawa, Y., Tremblay, R., Zhang, J., Feng, J. E., Sabol, A., … Lin, D. (2017). Esr1(+) cells in the ventromedial hypothalamus control female aggression. *Nature Neuroscience*, *20*(11), 1580–1590. https://doi.org/10.1038/nn.4644

Kruk, M. R., Van Der Poel, A. M., Meelis, W., Hermans, J., Mostert, P. G., Mos, J., & Lohman, A. H. M. (1983). Discriminant analysis of the localization of aggression-

inducing electrode placements in the hypothalamus of male rats. *Brain Research*. https://doi.org/10.1016/0006-8993(83)90764-3

Kunwar, P. S., Zelikowsky, M., Remedios, R., Cai, H., Yilmaz, M., Meister, M., & Anderson, D. J. (2015). Ventromedial hypothalamic neurons control a defensive emotion state. *ELife*, *4*, e06633. https://doi.org/10.7554/eLife.06633

Lee, H., Kim, D. W., Remedios, R., Anthony, T. E., Chang, A., Madisen, L., … Anderson, D. J. (2014). Scalable control of mounting and attack by Esr1+neurons in the ventromedial hypothalamus. *Nature*. https://doi.org/10.1038/nature13169

Leroy, F., Park, J., Asok, A., Brann, D. H., Meira, T., Boyle, L. M., … Siegelbaum, S. A. (2018). A circuit from hippocampal CA2 to lateral septum disinhibits social aggression. *Nature*, *564*(7735), 213–218. https://doi.org/10.1038/s41586-018-0772-0

Li, Y., Mathis, A., Grewe, B. F., Osterhout, J. A., Ahanonu, B., Schnitzer, M. J., … Dulac, C. (2017). Neuronal Representation of Social Information in the Medial Amygdala of Awake Behaving Mice. *Cell*, *171*(5), 1176–1190.e17. https://doi.org/10.1016/j.cell.2017.10.015

Lin, D., Boyle, M. P., Dollar, P., Lee, H., Lein, E. S., Perona, P., & Anderson, D. J. (2011). Functional identification of an aggression locus in the mouse hypothalamus. *Nature*. https://doi.org/10.1038/nature09736

Lo, L., Yao, S., Kim, D.-W., Cetin, A., Harris, J., Zeng, H., … Weissbourd, B. (2019). Connectional architecture of a mouse hypothalamic circuit node controlling social behavior. *Proceedings of the National Academy of Sciences of the United States of America*, *116*(15), 7503–7512. https://doi.org/10.1073/pnas.1817503116

Lorenz, K. (1963). *On aggression. On aggression.* Harcourt, Brace and World: New York.

Motta, S. C., Goto, M., Gouveia, F. V., Baldo, M. V. C., Canteras, N. S., & Swanson, L. W. (2009). Dissecting the brain's fear system reveals the hypothalamus is critical for responding in subordinate conspecific intruders. *Proceedings of the National Academy of Sciences*. https://doi.org/10.1073/pnas.0900939106

Olivier, B. (1977). The ventromedial hypothalamus and aggressive behaviour in rats. *Aggressive Behavior*, *3*(1), 47–56. https://doi.org/10.1002/1098-2337(1977)3:1<47::AID-AB2480030105>3.0.CO;2-H

Pedregosa, F., Varoquaux, G., Gramfort, A., Michel, V., Thirion, B., Grisel, O., … Duchesnay, É. (2012). Scikit-learn: Machine Learning in Python, 2825−2830. https://doi.org/10.1007/s13398-014-0173-7.2

Remedios, R., Kennedy, A., Zelikowsky, M., Grewe, B. F., Schnitzer, M. J., & Anderson, D. J. (2017). Social behaviour shapes hypothalamic neural ensemble representations of conspecific sex. *Nature*, *550*(7676), 388–392. https://doi.org/10.1038/nature23885

Risold, P. Y., & Swanson, L. W. (1997). Chemoarchitecture of the rat lateral septal nucleus. *Brain Research Reviews*. https://doi.org/10.1016/S0165-0173(97)00008-8

Sakurai, K., Zhao, S., Takatoh, J., Rodriguez, E., Lu, J., Leavitt, A. D., … Wang, F. (2016). Capturing and Manipulating Activated Neuronal Ensembles with CANE Delineates a Hypothalamic Social-Fear Circuit. *Neuron*, *92*(4), 739–753.

https://doi.org/10.1016/j.neuron.2016.10.015

Silva, B. A., Gross, C. T., & Graff, J. (2016). The neural circuits of innate fear: detection, integration, action, and memorization. *Learning & Memory (Cold Spring Harbor, N.Y.)*, *23*(10), 544–555. https://doi.org/10.1101/lm.042812.116

Silva, B. A., Mattucci, C., Krzywkowski, P., Cuozzo, R., Carbonari, L., & Gross, C. T. (2016). The ventromedial hypothalamus mediates predator fear memory. *The European Journal of Neuroscience*, *43*(11), 1431–1439. https://doi.org/10.1111/ejn.13239

Silva, B. A., Mattucci, C., Krzywkowski, P., Murana, E., Illarionova, A., Grinevich, V., … Gross, C. T. (2013). Independent hypothalamic circuits for social and predator fear. *Nat Neurosci*, *16*(12), 1731–1733. Retrieved from http://dx.doi.org/10.1038/nn.3573

Strange, B. A., Witter, M. P., Lein, E. S., & Moser, E. I. (2014). Functional organization of the hippocampal longitudinal axis. *Nature Reviews. Neuroscience*, *15*(10), 655–669. https://doi.org/10.1038/nrn3785

Swanson, L. W. (2000). Cerebral hemisphere regulation of motivated behavior. *Brain Research*. https://doi.org/10.1016/S0006-8993(00)02905-X

Swanson, L. W., & Petrovich, G. D. (1998). What is the amygdala? *Trends Neuroscience*. https://doi.org/10.1016/S0166-2236(98)01265-X

Tosches, M. A., & Arendt, D. (2013). The bilaterian forebrain: an evolutionary chimaera. *Current Opinion in Neurobiology*, *23*(6), 1080–1089. https://doi.org/10.1016/j.conb.2013.09.005

Viskaitis, P., Irvine, E. E., Smith, M. A., Choudhury, A. I., Alvarez-Curto, E., Glegola, J. A., … Withers, D. J. (2017). Modulation of SF1 Neuron Activity Coordinately Regulates Both Feeding Behavior and Associated Emotional States. *Cell Reports*, *21*(12), 3559–3572. https://doi.org/10.1016/j.celrep.2017.11.089

Wang, L., Talwar, V., Osakada, T., Kuang, A., Guo, Z., Yamaguchi, T., & Lin, D. (2019). Hypothalamic Control of Conspecific Self-Defense. *Cell Reports*, *26*(7), 1747–1758.e5. https://doi.org/10.1016/j.celrep.2019.01.078

Wong, L. C., Wang, L., D'Amour, J. A., Yumita, T., Chen, G., Yamaguchi, T., … Lin, D. (2016). Effective Modulation of Male Aggression through Lateral Septum to Medial Hypothalamus Projection. *Current Biology : CB*, *26*(5), 593–604. https://doi.org/10.1016/j.cub.2015.12.065

Yang, C. F., Chiang, M. C., Gray, D. C., Prabhakaran, M., Alvarado, M., Juntti, S. A., … Shah, N. M. (2013). Sexually dimorphic neurons in the ventromedial hypothalamus govern mating in both sexes and aggression in males. *Cell*. https://doi.org/10.1016/j.cell.2013.04.017

Yang, T., Yang, C. F., Chizari, M. D., Maheswaranathan, N., Burke, K. J. J., Borius, M., … Shah, N. M. (2017). Social Control of Hypothalamus-Mediated Male Aggression. *Neuron*, *95*(4), 955–970.e4. https://doi.org/10.1016/j.neuron.2017.06.046